Immunology
The Journal of cells, molecules, systems and technologies
British Society for immunology

IMMUNOLOGY ORIGINAL ARTICLE

Alteration of *N*-glycosylation in the kidney in a mouse model of systemic lupus erythematosus: relative quantification of *N*-glycans using an isotope-tagging method

Noritaka Hashii,[1,2] Nana Kawasaki,[1,2] Satsuki Itoh,[1] Yukari Nakajima,[1,2] Toru Kawanishi[1] and Teruhide Yamaguchi[1]

[1]*Division of Biological Chemistry and Biologicals, National Institute of Health Sciences, Setagaya-ku, Tokyo, Japan, and* [2]*Core Research for Evolutional Science and Technology (CREST) of the Japan Science and Technology Agency (JST), Kawaguchi City, Saitama, Japan*

doi:10.1111/j.1365-2567.2008.02898.x
Received 19 March 2008; revised 28 May 2008; accepted 2 June 2008.
Correspondence: N. Kawasaki, Division of Biological Chemistry and Biologicals, National Institute of Health Sciences, 1-18-1 Kamiyouga, Setagaya-ku, Tokyo 158-8501, Japan. Email: nana@nihs.go.jp
Senior author: Teruhide Yamaguchi, email: yamaguch@nihs.go.jp

Summary

Changes in the glycan structures of some glycoproteins have been observed in autoimmune diseases such as systemic lupus erythematosus (SLE) and rheumatoid arthritis. A deficiency of α-mannosidase II, which is associated with branching in *N*-glycans, has been found to induce SLE-like glomerular nephritis in a mouse model. These findings suggest that the alteration of the glycosylation has some link with the development of SLE. An analysis of glycan alteration in the disordered tissues in SLE may lead to the development of improved diagnostic methods and may help to clarify the carbohydrate-related pathogenic mechanism of inflammation in SLE. In this study, a comprehensive and differential analysis of *N*-glycans in kidneys from SLE-model mice and control mice was performed by using the quantitative glycan profiling method that we have developed previously. In this method, a mixture of deuterium-labelled *N*-glycans from the kidneys of SLE-model mice and non-labelled *N*-glycans from kidneys of control mice was analysed by liquid chromatography/mass spectrometry. It was revealed that the low-molecular-mass glycans with simple structures, including agalactobiantennary and paucimannose-type oligosaccharides, markedly increased in the SLE-model mouse. On the other hand, fucosylated and galactosylated complex type glycans with high branching were decreased in the SLE-model mouse. These results suggest that the changes occurring in the *N*-glycan synthesis pathway may cause the aberrant glycosylations on not only specific glycoproteins but also on most of the glycoproteins in the SLE-model mouse. The changes in glycosylation might be involved in autoimmune pathogenesis in the model mouse kidney.

Keywords: isotope-tagging method; liquid chromatography/multiple-stage mass spectrometry; systemic lupus erythematosus

Introduction

Glycosylation is one of the most common post-translational modifications[1,2] and contributes to many biological processes, including protein folding, secretion, embryonic development and cell–cell interactions.[3] Alteration of glycosylation is associated with several diseases, including inflammatory responses and malignancies;[4–6] for instance, significant increases in fucosylation and branching are found in ovarian cancer and lung cancer.[7] Additionally, the carbohydrate structure changes from type I glycans (Galβ1-3GlaNAc) to type II glycans (Galβ1-4GalNAc) in carcinoembryonic antigen in colon cancer.[8] Furthermore, an increase in biantennary oligosaccharides lacking galactose (Gal) was found on immunoglobulin G (IgG) in systemic lupus erythematosus (SLE) and rheumatoid arthritis,[9–11] and agalactoglycans are used for the early diagnosis of rheumatoid arthritis.[12]

Systemic lupus erythematosus is an autoimmune disease characterized as chronic and as a systemic disease, with symptoms such as kidney failure, arthritis and erythema. In addition to the known changes in glycosylation on IgG, there have been several reports on the association between glycosylation and inflammation in SLE and rheumatoid

arthritis.[13–15] A deficiency of α-mannosidase II (αM-II), which is associated with branching in *N*-glycans, has been found to induce human SLE-like glomerular nephritis in a mouse model.[16] Green *et al.* reported that branching structures of *N*-glycan in mammals are involved in protection against immune responses in autoimmune disease pathogenesis.[17] Although there is no direct evidence that alteration of glycosylation is the upstream event in the pathogenesis of SLE, these findings suggest that changes in the glycan structure may be involved in the inflammatory-related autoimmune disorder. Glycosylation analysis may lead to the development of improved diagnostic methods and may help to clarify the carbohydrate-related pathogenic mechanism of inflammation in SLE.

Mass spectrometry (MS) and liquid chromatography/mass spectrometry (LC/MS) are the most prevalent strategies for identifying disease-related glycans in glycomics.[18–20] Aberrant glycosylations in some disease samples have been found by comparing mass spectra or chromatograms between normal and disease samples; however, because of the tremendous heterogeneities of the sugar moiety in glycoprotein as well as the low reproducibility of LC/MS, accurate quantitative analysis is difficult using MS and LC/MS alone. To overcome these problems, we previously developed the stable isotope-tagging method for the quantitative profiling of glycans using 2-aminopyridine (AP).[21] After the glycans are released from sample and the reference glycoproteins are derivatized to pyridyl amino (d_0-PA) glycans and to tetra-deuterium-labelled pyridyl amino (d_4-PA) glycans, respectively, a mixture of both d_0-PA and d_4-PA glycans was subjected to LC/MS, and the levels of individual glycans were calculated from the intensity ratios of d_0-glycan and d_4-glycan molecular ions (Fig. 1a). Recently, alternative isotope-tagging methods using deuterium-labelled compounds, such as 2-aminobenzoic acid its derivatives, and permethylation, have been proposed by other groups.[22–24] All of these studies prove the utility of isotope-tagging methods for the quantitative analysis of glycosylation.

In the present study, we used the isotope-tagging method to analyse changes in *N*-glycosylation in the disordered kidney in an SLE mouse model. We used an MRL/MpJ-lpr/lpr (MRL-lpr) mouse which lacks the Fas antigen gene.[25–27] The MRL-lpr mouse is known to naturally develop SLE-like glomerular nephritis and is widely used in SLE studies. MRL/MpJ-+/+ (MRL-+/+) mice were used as controls.

Materials and methods

Materials

The kidneys of the SLE-model mice (MRL-lpr) and control mice (MRL-+/+) (n = 3) were purchased from Japan SLC, Inc. (Hamamatsu, Japan). Thermolysin (EC 3.4.24.27), originating from *Bacillus thermoproteolyticus*

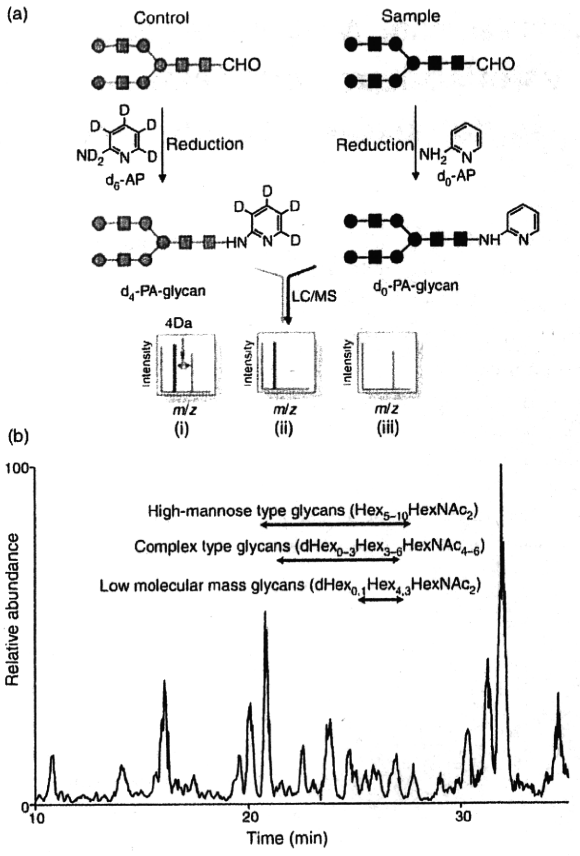

Figure 1. (a) Quantitative glycan profiling using the stable isotope-tagging method and liquid chromatography/mass spectrometry (LC/MS). (i) sample = control, (ii) sample > control, (iii) sample < control. (b) Total ion chromatogram obtained by a single scan (m/z 700–2000) of the d_0-glycan and d_4-glycan mixture.

Rokko, was purchased from Daiwa Kasei (Shiga, Japan). Glycopeptidase A (PNGase A) was obtained from Seikagaku Kogyo Corporation (Tokyo, Japan). Non-deuterium-labelled 2-aminopyridine (d_0-AP) and deuterium-labelled 2-aminopyridine (d_6-AP) were purchased from Takara Bio (Otsu, Japan) and Cambridge Isotope Laboratories (Andover, MA), respectively.

Sample preparation

Mouse kidneys were filtered using a cell strainer (70 μm; BD Biosciences, San Jose, CA) and contaminating blood cells in the kidney cells were burst in 140 mM NH_4Cl–Tris buffer (pH 7·2). The surviving kidney cells were washed three times with phosphate-buffered saline containing a mixture of protease inhibitors (Wako, Tokyo, Japan) and dissolved in guanidine–HCl buffer (8 M guanidine–HCl, 0·5 M Tris–HCl, pH 8·6) containing a mixture of protease inhibitors by vortexing at 4°. The protein concentration was measured using a 2-D Quant Kit (GE Healthcare

Bio-Sciences, Uppsala, Sweden). The protein solution (200 μg proteins) was incubated with 40 mM dithiothreitol at 65° for 30 min. Freshly prepared sodium iodoacetate (final concentration, 96 mM) was added to the sample solution, and the mixture was incubated at room temperature for 40 min in the dark. The reaction was stopped by adding cystine (6 mg/ml in 2 M HCl) in an amount equal to the amount of dithiothreitol. The solution containing carboxymethylated proteins was diluted in four times its volume of H_2O, and the mixture was incubated with 0·1 μg of thermolysin at 65° for 1 hr. After terminating the reaction by boiling, the reaction mixture was diluted in four times its volume of 0·2 M acetate buffer. The *N*-linked glycans were released by treatment with PNGase A (1 mU) at 37° for 16 hr and were desalted using an EnviCarb C cartridge (Supelco, Bellefonte, PA).

Labelling of N-glycans with d_0-AP and d_6-AP

Glycans released from the SLE-model mouse cells were incubated in acetic acid (20 μl) with 12·5 M d_0-AP at 90° for 1 hr. Next, 3·3 M borane–dimethylamine complex reducing reagent in acetic acid (20 μl) was added to the solution and the mixture was incubated at 80° for 1 hr. Excess reagent was removed by evaporation, and d_0-PA glycans were desalted using an EnviCarb C cartridge, concentrated in a SpeedVac and reconstituted in 20 μl of 5 mM ammonium acetate (pH 9·6). Glycans released from the control mouse were labelled with d_6-AP in a similar manner. The resulting d_4-PA glycans were combined with d_0-PA glycans, which were prepared from an equal amount of proteins.

On-line liquid chromatography/mass spectrometry

The sample solution (4 μl) was injected into the LC/MS system through a 5-μl capillary loop. The d_0-PA and d_4-PA glycans were separated in a graphitized carbon column (Hypercarb, 150 × 0·2 mm, 5 μm; Thermo Fisher Scientific, Waltham, MA) at a flow rate of 2 μl/min in a Magic 2002 LC system (Michrom Bioresources, Auburn, CA). The mobile phases were 5 mM ammonium acetate containing 2% acetonitrile (pH 9·6, A buffer) and 5 mM ammonium acetate containing 90% acetonitrile (pH 9·6, B buffer). The PA-glycans were eluted with a linear gradient of 5–45% of B buffer for 90 min.

Mass spectrometric analysis of PA glycans was performed using a Fourier transform ion cyclotron resonance/ion trap mass spectrometer (FT-ICR-MS, LTQ-FT; Thermo Fisher Scientific) equipped with a nanoelectrospray ion source (AMR, Tokyo, Japan). For MS, the electrospray voltage was 2·0 kV in the positive ion mode, the capillary temperature was 200°, the collision energy was 25% for MS^n experiment, and the maximum injection times for FT ICR-MS and MS^n were 1250 and 50 milliseconds, respectively. The resolution of FT-ICR-MS was 50 000, the scan time (*m/z* 700–2000) was approximately 0·2 seconds, dynamic exclusion was 18 seconds, and the isolation width was 3·0 U (range of precursor ions ± 1·5).

Results

Quantitative profiling of kidney oligosaccharides in the SLE-model mouse

The recovery of oligosaccharides from whole tissues and cells is generally low because of the insolubility of the membrane fraction and possible degradation of the glycans. To improve the recovery of *N*-glycans from kidney cells, whole cells were dissolved in guanidine hydrochloride solution, and all proteins, including membrane proteins, were digested into peptides and glycopeptides with thermolysin. The *N*-glycans were then released from the glycopeptides with PNGase A, which is capable of liberating *N*-linked oligosaccharides even at the N- and/or C-terminals of peptides. The *N*-linked oligosaccharides from the SLE-model mice and control mice were labelled with d_0-AP and d_6-AP, respectively. The mixture of labelled glycans derived from an equal amount of proteins was subjected to quantitative glycan profiling using LC/MS^n.

Figure 1(b) shows the total ion chromatogram obtained by a single mass scan (*m/z* 700–2000) of the glycan mixture in the positive ion mode. Although the MS data contain many MS spectra derived from contaminating low-molecular-weight peptides, the MS/MS spectra of oligosaccharides could be sorted based on the existence of carbohydrate-distinctive ions, such as $HexHexNAc^+$ (*m/z* 366) and $Hex(dHex)HexNAc^+$ (*m/z* 512). The monosaccharide compositions of the precursor ions were calculated from accurate *m/z* values acquired by FT-ICR-MS. Oligosaccharides found at 25–27 min were assigned to low-molecular-mass glycans consisting of $dHex_{0,1}Hex_{4,3}HexNAc_2$ (dHex, deoxyhexose; Hex, hexose; HexNAc, *N*-acetylhexosamine). High-mannose-type glycans, which consist of $Hex_{5-10}HexNAc_2$, were located at 20–28 min; complex-type glycans ($dHex_{0-3}Hex_{3-6}HexNAc_{4-6}$) were found at 21–27 min. Figure 2(a) shows the relative intensities of the molecular ions of *N*-glycans in the SLE-model mouse, which may correspond roughly to the levels of individual *N*-glycans. More than half of all glycans were complex-type oligosaccharides, and the most prominent glycan was $dHex_3Hex_5HexNAc_5$. Man-9 ($Hex_9HexNAc_2$) was the second most common oligosaccharide. Nearly one-quarter of the glycans were low-molecular-mass glycans, and $dHex_1Hex_2HexNAc_2$ was the third most abundant glycan in the SLE-model mouse. The rate of percentage change in individual glycans between the SLE-model mice and control mice was calculated from the intensity ratio of d_0-glycan and d_4-glycan

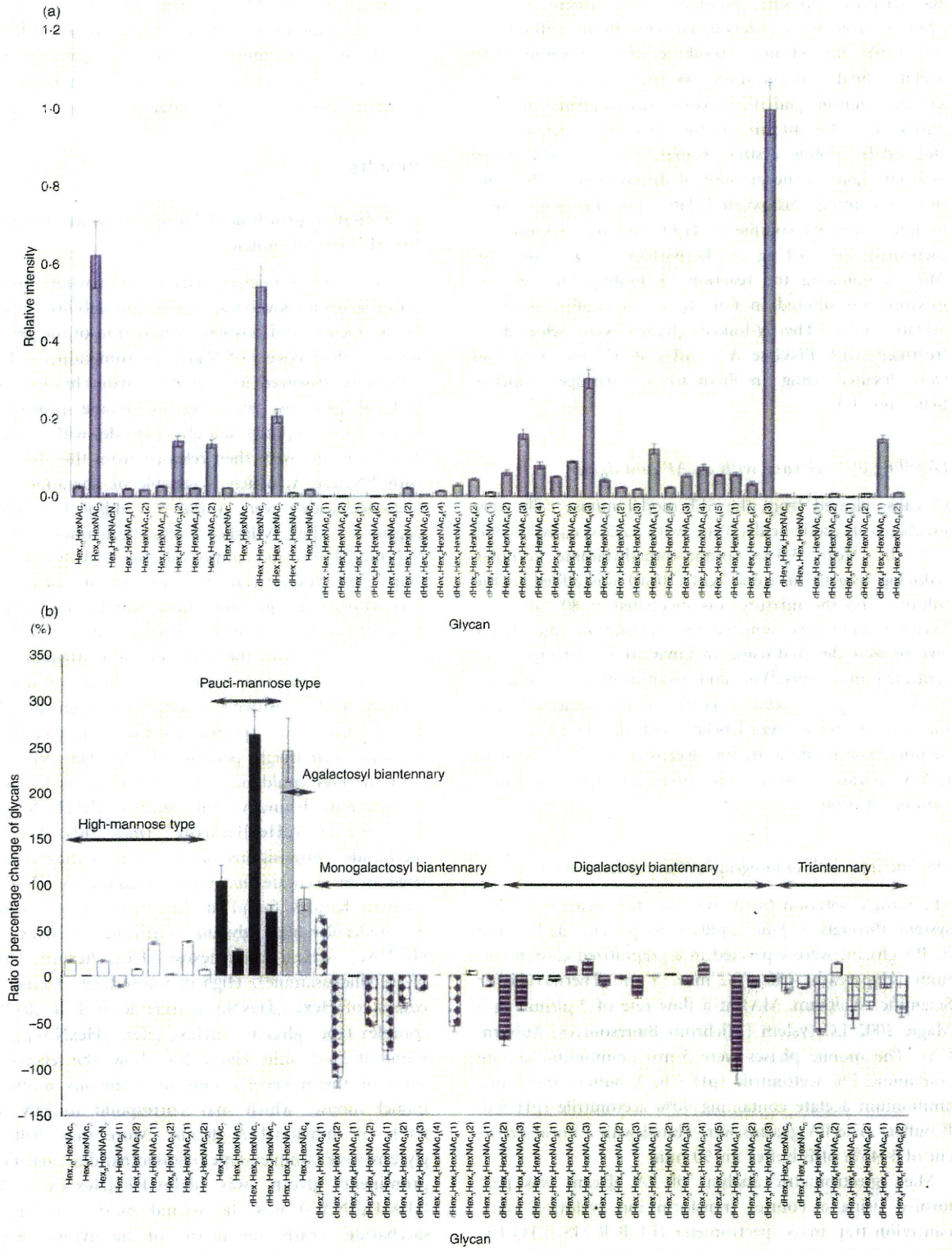

Figure 2. (a) Relative intensities of the molecular ions of d_0-pyridyl amino (PA) glycans from the systemic lupus erythematosus (SLE) model mouse. The intensity of the most intense ion ($[M + 2H]^{2+}$of d_4-PA $dHex_3Hex_5HexNAc_3(3)$, *m/z* 1180·97) was taken as 1·0. (b) Rate of percentage change of d_0/d_4-glycans. Each value is the average of three biological repeats. Error bars correspond to the standard deviation. The numbers in parentheses show the isomers.

molecular ions (Fig. 2b). The significant changes found in many glycans are described below.

Increased oligosaccharides in the SLE-model mouse

Figure 3(a,b) show the mass and MS/MS spectra of the most increased glycan, which showed a notable increase in the SLE-model mouse. Based on *m/z* values of molecular ions and differences of 1·00 U in *m/z* values among monoisotopic ions, the intense ion (*m/z* 973·40) and its neighbour ion (*m/z* 977·43) were assigned to $[M+H]^+$ of d_0-PA $dHex_1Hex_2HexNAc_2$, and d_4-PA $dHex_1Hex_2HexNAc_2$, respectively (Fig. 3a). The intensity ratio of these ions suggested that the level of $dHex_1Hex_2HexNAc_2$ increased 3·6-fold in the SLE-model mouse. The structure of this oligosaccharide was estimated to be a core-fucosylated trimannosyl core lacking a Man residue from the successive cleavages of Man (Y_3: *m/z* 815), Man (Y_2: *m/z* 653), GlcNAc (Y_1: *m/z* 450) and Fuc ($Y_{1/1'}$: *m/z* 304) (inset in Fig. 3b). Such a defective *N*-glycan is known as a paucimannose-type glycan, and is rarely found in vertebrates. All paucimannose-type glycans, such as $dHex_1Hex_3HexNAc_2$ (a core-fucosylated trimannosyl core) and $Hex_3HexNAc_2$ (a non-fucosylated trimannosyl core) were increased in the SLE-model mouse. Furthermore, a two-fold increase was found in $Hex_4HexNAc_2$ (Man-4).

Figure 4 shows the molecular ratios of individual *N*-glycans between the SLE-model mice and control mice. A remarkable increase (3·5-fold) was also found in $dHex_1Hex_3HexNAc_4$, which is assigned to a core-fucosylated biantennary oligosaccharide lacking two non-reducing terminal Gal residues; its non-fucosylated form ($Hex_3HexNAc_4$) was also increased 1·8-fold in the SLE-model mouse. In other complex-type glycans, $dHex_1Hex_4HexNAc_4$ (1), which is assigned to a biantennary oligosaccharide lacking one molecule of Gal, increased 1·6-fold. Interestingly, a significant decrease was found in $dHex_1Hex_4HexNAc_4$ (2), a positional isomer of $dHex_1Hex_4HexNAc_4$ (1); this might have been caused by galactosylation on either GlcNAc-Manα1–3 or GlcNAc-Manα1–6. In contrast, no change was found between fucosylated and non-fucosylated oligosaccharides, nor between bisected and non-bisected oligosaccharides.

A significant increase was found in some high-mannose-type oligosaccharides, such as $Hex_5HexNAc_2$ (Man-5; + 137%) and $Hex_6HexNAc_2$ (1) (Man-6; + 136%), while $Hex_7HexNAc_2$ (1,2) (Man-7) and a positional isomer of $Hex_6HexNAc_2$ (1) [$Hex_6HexNAc_2$ (2)] remained unchanged in the SLE-model mouse. A slight increase was found in $Hex_8HexNAc_2$ (Man-8; + 116%) and $Hex_{10}HexNAc_2$ (possibly assigned to Man-9 plus Glc; + 116%).

Decreased oligosaccharides in the SLE-model mouse

The mass spectrum of the most decreased glycan is shown in Fig. 5(a). Based on differences of 0·5 U in *m/z* values among monoisotopic ions, molecular ions at *m/z* 1180·97

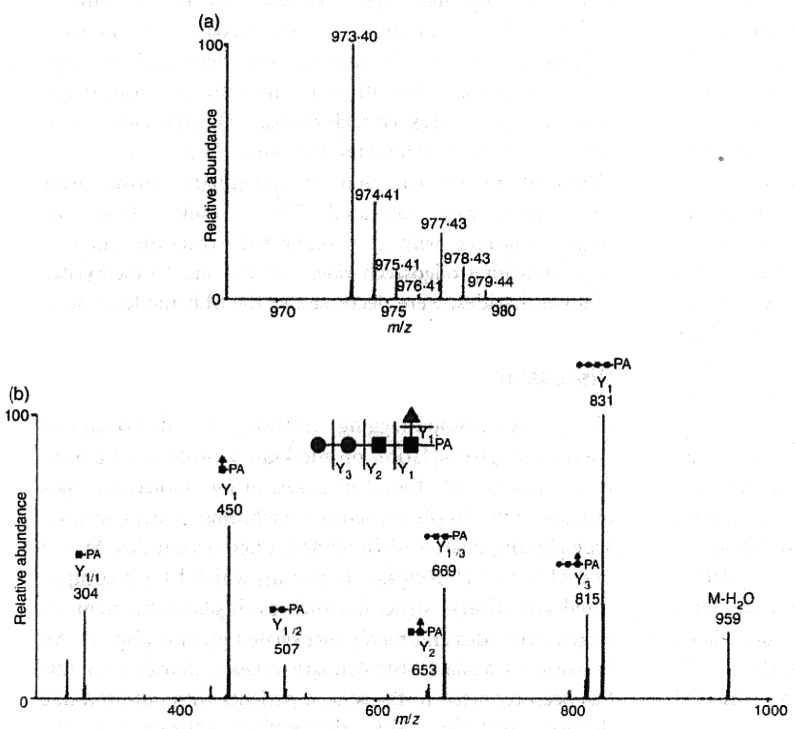

Figure 3. Mass (a) and mass spectrometry (MS)/MS (b) spectra of the most increased glycan ($dHex_1Hex_3HexNAc_2$). Precursor ion, *m/z* 973·4; grey circle, mannose; grey triangle, fucose; black square, *N*-acetylglucosamine.

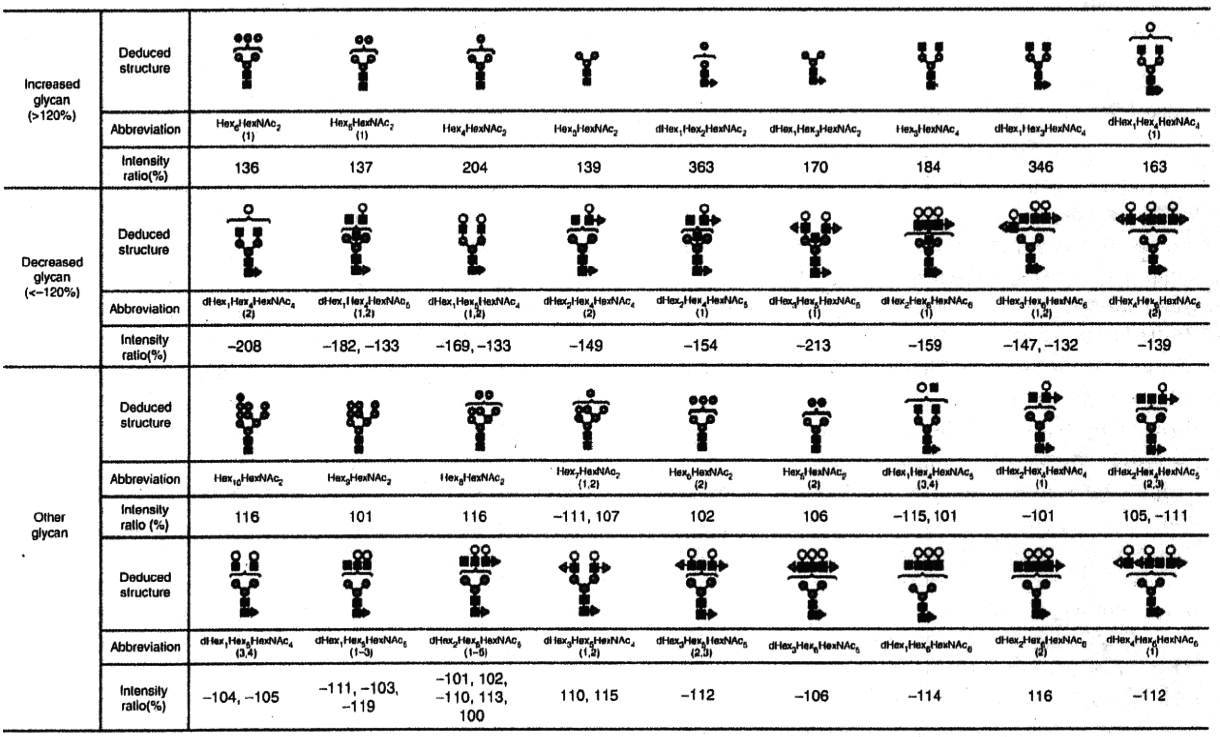

Figure 4. Summary of quantitative analysis of the systemic lupus erythematosus (SLE) model mouse against control mice. Values of relative ratios are the averages of three biological repeats. Grey circle, mannose; white circle, galactose; grey triangle, fucose; black square, *N*-acetylglucosamine.

and 1182·98 are estimated to be $[M + 2H]^{2+}$ of d_0-PA and d_4-PA $dHex_3Hex_5HexNAc_5$ (1), respectively. The intensity ratio of $d_0 : d_4$ glycans suggests that this glycan in the SLE-model mouse was decreased to 47% of the amount found in the control mouse. Figure 5(b) shows the MS^{2-4} spectra of d_0-PA $dHex_3Hex_5HexNAc_5$ (1) (precursor ion, *m/z* 1180·97). The fragment ion at *m/z* 512 in MS/MS (i) and MS/MS/MS (ii) spectra, which corresponds to $dHex_1Hex_1HexNAc_1^+$, suggests the attachment of two Lewis motifs on the side chains of the glycan. The presence of $dHex_1HexNAc_1PA^+$ (*m/z* 446) and $dHex_1Hex_1HexNAc_3PA^+$ (*m/z* 1015) reveals the linkages of a core fucose and a bisecting GlcNAc. Based on these fragments, this decreased glycan is estimated to be a Lewis-motif-modified, core-fucosylated and bisected biantennary oligosaccharide (inset in Fig. 5).

As shown in Figs 2(b) and 4, oligosaccharides lacking one molecule of Gal with and without bisecting GlcNAc [$dHex_1Hex_4HexNAc_4$ (2) and $dHex_1Hex_4HexNAc_5$ (1)] were decreased to 48% and 55%, respectively. A significant decrease was also found in other monogalactobiantennary oligosaccharides, such as $dHex_2Hex_4HexNAc_4$ (2) (a Lewis-motif-modified, core-fucosylated monogalacto-biantennary) and $dHex_2Hex_4HexNAc_5$ (1) (a Lewis-motif-modified core-fucosylated and bisected monogalacto-biantennary).

The oligosaccharides, non-reducing ends of which are fully galactosylated, were decreased in the SLE-model mouse. For example, monofucosyl biantennary $dHex_1Hex_5HexNAc_4$ (1) and (2) were decreased 59% and 75%, respectively. The di-, tri- and tetra-fucosylated oligosaccharides, $dHex_2Hex_6HexNAc_6$ (1), $dHex_3Hex_6HexNAc_6$ (1,2) and $dHex_4Hex_6HexNAc_6$ (1,2), which were estimated to be tri- and tetraantennary forms, were also significantly decreased. These results show that oligosaccharides with a complicated structure, such as high branching oligosaccharides and di- and tri-fucosylated oligosaccharides, were decreased in the SLE-model mouse.

Discussion

Using the isotope-tagging method, we demonstrated aberrant *N*-glycosylation on the kidney proteins of a SLE-model mouse. We found increases in low-molecular-mass glycans with simple structures, including paucimannose-type glycans, agalacto-biantennary oligosaccharides, Man-5 and Man-6, and decreases in glycans which have a complicated and diverse structure, such as digalacto-biantennary oligosaccharides and highly fucosylated glycans (Fig. 4). An increase in agalacto-biantennary oligosaccharides on IgG has been reported in the sera of patients with autoimmune diseases, including SLE, rheumatoid arthritis and IgA

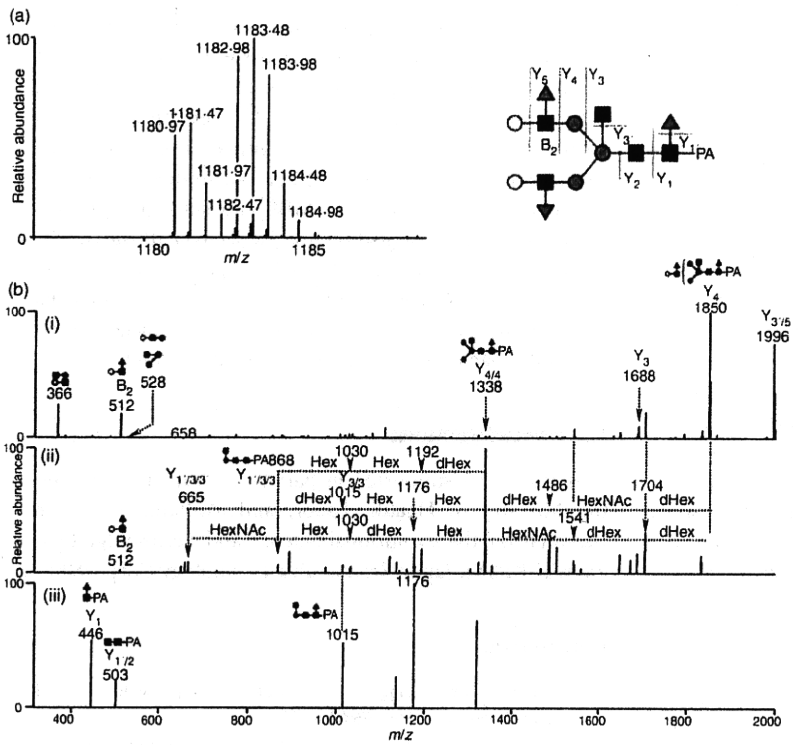

Figure 5. (a) Mass spectrum of the most decreased glycan [$dHex_3Hex_5HexNAc_5$ (1)]; (b-i) Mass spectrometry (MS)/MS spectrum of *m/z* 1181·0; (b-ii) MS/MS/MS spectrum of *m/z* 1849·7; (b-iii) MS/MS/MS/MS spectrum of *m/z* 1338·3. Grey circle, mannose; white circle, galactose; grey triangle, fucose; black square, *N*-acetylglucosamine; dHex, deoxyhexose (fucose); Hex, hexose (mannose and galactose); HN, *N*-acetylhexosamine (*N*-acetylglucosamine).

nephropathy.[9,11,28] The present findings show that abnormal glycosylation occurs not only in IgG in serum but also in several glycoproteins in the SLE-model mouse kidney.

Figure 6 shows the biosynthesis pathway of *N*-linked oligosaccharides in mammalian cells. Man-9, a product in the early stage of the pathway, is processed to Man-5 in the endoplasmic reticulum, and a GlcNAc and Fuc are added to Man-5 in the Golgi apparatus. After the removal of two Man residues by αM-II, GlcNAc, Gal and Fuc are further added to oligosaccharides by several glycosyltransferases. There have been a few reports on paucimannose-type oligosaccharides in vertebrates;[29] however, these glycans are common oligosaccharides in other multicellular organisms such as insects and *Caenorhabditis elegans*.[30,31] The membrane protease β-*N*-acetylglucosaminidase is thought to mediate the synthesis of paucimannose-type oligosaccharides.[32] Based on core fucosylation on some paucimannose-type oligosaccharides, it was deduced that β-*N*-acetylglucosaminidase might act on glycan synthesis after *N*-acetylglucosaminyltransferase I, core fucosyltransferase and αM-II.[32] The synthesis of paucimannose-type oligosaccharides may be involved in the suppression of growing diversity and complexity of glycan structures.

We found a number of changes in the levels of monogalacto-biantennary oligosaccharides in the SLE mouse. Galactosylation to agalacto-biantennary oligosaccharides is mediated by β-1,4-galactosyltransferase

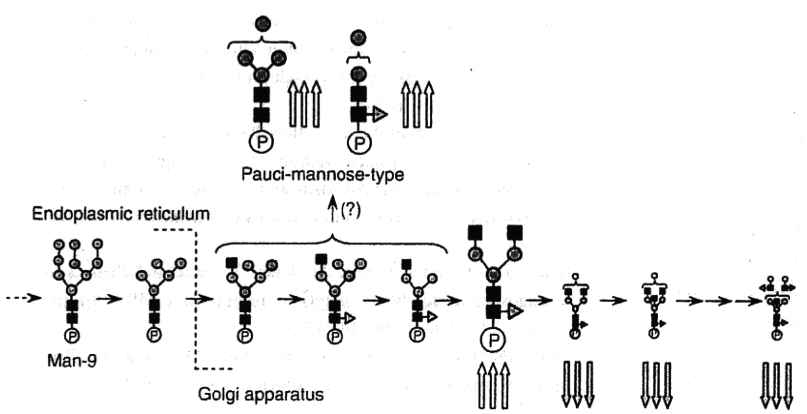

Figure 6. Biosynthesis pathway of *N*-linked oligosaccharides in mammalian cells. Triple up-arrow, increases of more than +2·0; triple down-arrow, decreases of not more than −2·0. Grey circle, mannose; white circle, galactose; grey triangle, fucose; black square, *N*-acetylglucosamine. 'P' is protein portion.

(β-1,4-GalTase).[33] Previous studies suggested that translational repression of β-1,4-GalTase in lymphocytes is associated with an increase in agalacto-oligosaccharides on IgG in the serum of the MRL-lpr mouse.[34] Although the activity of β-1,4-GalTase remains unknown in the SLE-model mouse, the increase in agalacto forms and the decrease in digalacto forms imply changes in β-1,4-GalTase activity. The present results suggest a decrease in diverse and complex glycans, which are synthesized at a late stage in the *N*-glycan synthesis pathway, and an increase in the simple glycans appearing at an early stage in the SLE-model mouse.

The activation of complements is involved in glomerular nephritis of SLE.[35–37] The complements are activated through three pathways: a classical pathway, an alternative pathway and a lectin pathway. In the classical pathway, a binding of C1q to an immune complex triggers the activation of C1r and C1s. Activated C1s cleaves C4 and C2, generating C3 convertase (C4b2a), which generates C3b. The complement component subsequently produces C5b-9 complex, which leads to an inflammatory response on host tissues.[38–41] The excess deposition of immune complexes followed by a sustained immune response triggers tissue disorders, including lupus nephritis.[42–45] In the lectin pathway, mannose-binding lectin (MBL) is associated with the activation of complements. Two forms of MBL (MBL-A and MBL-C) are present in complexes with MBL-associated serine proteases (MASPs) in mice. The MASPs are activated by binding MBL to Man or GlcNAc on the surface of the antigen in a calcium-dependent manner.[46–49] Like C1s in the classical pathway, activated MASPs cleave C4 and C2.[50,51] In lupus nephritis, MBL-A and MBL-C in the immune complex bind to GlcNAc residues at the reducing ends of agalacto-biantennary oligosaccharides in IgG,[52] and subsequently activate the complements.[53,54] In αM-II-deficient mice, which suffer from SLE-like syndromes including kidney disorders, the majority of glycans are hybrid-type oligosaccharides because of the failure of Man trimming by the lack of αM-II.[16] Green *et al.* concluded that MBL recognized Manα1–3 and Manα1–6 linkages in hybrid-type oligosaccharides,[17] and glycans lacking normal side chains, including agalacto-biantennary oligosaccharides, might be involved in the aberrant immune response in autoimmune diseases. Paucimannose glycans, which contain exposed Manα1–3 or Manα1–6 linkages, may be recognized as ligand carbohydrates by MBL. Our present finding, an increase in paucimannose oligosaccharides and agalacto forms, might result from an alteration of the biosynthesis pathway of *N*-glycans. The alterations may cause the aberrant glycosylations on most of the glycoproteins rather than some glycoproteins in the SLE-model mouse. The changes in glycosylation might be involved in an autoimmune pathogenesis in the SLE-model mouse kidney.

The continuous production of aberrant antibodies that react with components from self-tissue and accumulation in the immune complex are thought to promote tissue damage in autoimmune disease.[55,56] The mechanism of localized accumulation in the immune complex in some tissues remains unknown in SLE. We found an increase in glycans that may bind to MBL and subsequently promote complement activation via the lectin pathway in the mouse kidney. Our present results suggest that an aberrant *N*-glycan synthesis pathway as well as an abnormal immune system may be involved in the damage caused by glomerular nephritis in the SLE-model mouse.

Acknowledgements

This study was supported in part by a Grant-in-Aid from the Ministry of Health, Labor, and Welfare, and Core Research for the Evolutional Science and Technology Program (CREST), Japan Science and Technology Corp (JST).

References

1 Dwek RA. Glycobiology: toward understanding the function of sugars. *Chem Rev* 1996; **96**:683–720.
2 Helenius A, Aebi M. Intracellular functions of N-linked glycans. *Science* 2001; **291**:2364–9.
3 Zak I, Lewandowska E, Gnyp W. Selectin glycoprotein ligands. *Acta Biochim Pol* 2000; **47**:393–412.
4 Axford JS. Glycosylation and rheumatic disease. *Biochim Biophys Acta* 1999; **1455**:219–29.
5 Feizi T, Gooi HC, Childs RA, Picard JK, Uemura K, Loomes LM, Thorpe SJ, Hounsell EF. Tumour-associated and differentiation antigens on the carbohydrate moieties of mucin-type glycoproteins. *Biochem Soc Trans* 1984; **12**:591–6.
6 Kannagi R, Izawa M, Koike T, Miyazaki K, Kimura N. Carbohydrate-mediated cell adhesion in cancer metastasis and angiogenesis. *Cancer Sci* 2004; **95**:377–84.
7 Goodarzi MT, Turner GA. Decreased branching, increased fucosylation and changed sialylation of alpha-1-proteinase inhibitor in breast and ovarian cancer. *Clin Chim Acta* 1995; **236**:161–71.
8 Yamashita K, Fukushima K, Sakiyama T, Murata F, Kuroki M, Matsuoka Y. Expression of Sia alpha 2→6Gal beta 1→4GlcNAc residues on sugar chains of glycoproteins including carcinoembryonic antigens in human colon adenocarcinoma: applications of *Trichosanthes japonica* agglutinin I for early diagnosis. *Cancer Res* 1995; **55**:1675–9.
9 Tomana M, Schrohenloher RE, Reveille JD, Arnett FC, Koopman WJ. Abnormal galactosylation of serum IgG in patients with systemic lupus erythematosus and members of families with high frequency of autoimmune diseases. *Rheumatol Int* 1992; **12**:191–4.
10 Mizuochi T, Hamako J, Nose M, Titani K. Structural changes in the oligosaccharide chains of IgG in autoimmune MRL/Mp-lpr/lpr mice. *J Immunol* 1990; **145**:1794–8.
11 Arnold JN, Wormald MR, Sim RB, Rudd PM, Dwek RA. The impact of glycosylation on the biological function and structure

of human immunoglobulins. *Annu Rev Immunol* 2007; **25**:21–50.

12 Das H, Atsumi T, Fukushima Y *et al.* Diagnostic value of anti-agalactosyl IgG antibodies in rheumatoid arthritis. *Clin Rheumatol* 2004; **23**:218–22.

13 Raghav SK, Gupta B, Agrawal C, Saroha A, Das RH, Chaturvedi VP, Das HR. Altered expression and glycosylation of plasma proteins in rheumatoid arthritis. *Glycoconj J* 2006; **23**:167–73.

14 Elliott MA, Elliott HG, Gallagher K, McGuire J, Field M, Smith KD. Investigation into the concanavalin A reactivity, fucosylation and oligosaccharide microheterogeneity of alpha 1-acid glycoprotein expressed in the sera of patients with rheumatoid arthritis. *J Chromatogr B Biomed Sci Appl* 1997; **688**:229–37.

15 Rops AL, van den Hoven MJ, Bakker MA *et al.* Expression of glomerular heparan sulphate domains in murine and human lupus nephritis. *Nephrol Dial Transplant* 2007; **22**:1891–902.

16 Chui D, Sellakumar G, Green R *et al.* Genetic remodeling of protein glycosylation *in vivo* induces autoimmune disease. *Proc Natl Acad Sci USA* 2001; **98**:1142–7.

17 Green RS, Stone EL, Tenno M, Lehtonen E, Farquhar MG, Marth JD. Mammalian *N*-glycan branching protects against innate immune self-recognition and inflammation in autoimmune disease pathogenesis. *Immunity* 2007; **27**:308–20.

18 Wada Y. Mass spectrometry in the detection and diagnosis of congenital disorders of glycosylation. *Eur J Mass Spectrom (Chichester, Eng)* 2007; **13**:101–3.

19 Faid V, Chirat F, Seta N, Foulquier F, Morelle W. A rapid mass spectrometric strategy for the characterization of *N*- and *O*-glycan chains in the diagnosis of defects in glycan biosynthesis. *Proteomics* 2007; **7**:1800–13.

20 Miyamoto S. Clinical applications of glycomic approaches for the detection of cancer and other diseases. *Curr Opin Mol Ther* 2006; **8**:507–13.

21 Yuan J, Hashii N, Kawasaki N, Itoh S, Kawanishi T, Hayakawa T. Isotope tag method for quantitative analysis of carbohydrates by liquid chromatography-mass spectrometry. *J Chromatogr A* 2005; **1067**:145–52.

22 Alvarez-Manilla G, Warren NL, Abney T, Atwood J III, Azadi P, York WS, Pierce M, Orlando R. Tools for glycomics: relative quantitation of glycans by isotopic permethylation using 13CH3I. *Glycobiology* 2007; **17**:677–87.

23 Kang P, Mechref Y, Kyselova Z, Goetz JA, Novotny MV. Comparative glycomic mapping through quantitative permethylation and stable-isotope labeling. *Anal Chem* 2007; **79**:6064–73.

24 Bowman MJ, Zaia J. Tags for the stable isotopic labeling of carbohydrates and quantitative analysis by mass spectrometry. *Anal Chem* 2007; **79**:5777–84.

25 Watanabe-Fukunaga R, Brannan CI, Copeland NG, Jenkins NA, Nagata S. Lymphoproliferation disorder in mice explained by defects in Fas antigen that mediates apoptosis. *Nature* 1992; **356**:314–7.

26 Adachi M, Watanabe-Fukunaga R, Nagata S. Aberrant transcription caused by the insertion of an early transposable element in an intron of the Fas antigen gene of lpr mice. *Proc Natl Acad Sci USA* 1993; **90**:1756–60.

27 Merino R, Iwamoto M, Fossati L, Izui S. Polyclonal B cell activation arises from different mechanisms in lupus-prone (NZB × NZW)F_1 and MRL/MpJ-lpr/lpr mice. *J Immunol* 1993; 151:6509–16.

28 Homma H, Tozawa K, Yasui T, Itoh Y, Hayashi Y, Kohri K. Abnormal glycosylation of serum IgG in patients with IgA nephropathy. *Clin Exp Nephrol* 2006; **10**:180–5.

29 Hase S, Okawa K, Ikenaka T. Identification of the trimannosylchitobiose structure in sugar moieties of Japanese quail ovomucoid. *J Biochem* 1982; **91**:735–7.

30 Kubelka V, Altmann F, Kornfeld G, Marz L. Structures of the N-linked oligosaccharides of the membrane glycoproteins from three lepidopteran cell lines (Sf-21, IZD-Mb-0503, Bm-N). *Arch Biochem Biophys* 1994; **308**:148–57.

31 Natsuka S, Adachi J, Kawaguchi M, Nakakita S, Hase S, Ichikawa A, Ikura K. Structural analysis of N-linked glycans in *Caenorhabditis elegans*. *J Biochem* 2002; **131**:807–13.

32 Altmann F, Schwihla H, Staudacher E, Glossl J, Marz L. Insect cells contain an unusual, membrane-bound beta-*N*-acetylglucosaminidase probably involved in the processing of protein *N*-glycans. *J Biol Chem* 1995; **270**:17344–9.

33 Guo S, Sato T, Shirane K, Furukawa K. Galactosylation of N-linked oligosaccharides by human beta-1,4-galactosyltransferases I, II, III, IV, V, and VI expressed in Sf-9 cells. *Glycobiology* 2001; **11**:813–20.

34 Jeddi PA, Lund T, Bodman KB *et al.* Reduced galactosyltransferase mRNA levels are associated with the agalactosyl IgG found in arthritis-prone MRL-lpr/lpr strain mice. *Immunology* 1994; **83**:484–8.

35 Cameron JS. Lupus nephritis. *J Am Soc Nephrol* 1999; **10**:413–24.

36 Walport MJ. Complement. First of two parts. *N Engl J Med* 2001; **344**:1058–66.

37 Walport MJ. Complement. Second of two parts. *N Engl J Med* 2001; **344**:1140–4.

38 Botto M. Links between complement deficiency and apoptosis. *Arthritis Res* 2001; **3**:207–10.

39 Hanayama R, Tanaka M, Miyasaka K, Aozasa K, Koike M, Uchiyama Y, Nagata S. Autoimmune disease and impaired uptake of apoptotic cells in MFG-E8-deficient mice. *Science* 2004; **304**:1147–50.

40 Arason GJ, Steinsson K, Kolka R, Vikingsdottir T, D'Ambrogio MS, Valdimarsson H. Patients with systemic lupus erythematosus are deficient in complement-dependent prevention of immune precipitation. *Rheumatology (Oxford)* 2004; **43**:783–9.

41 Cook HT, Botto M. Mechanisms of disease: the complement system and the pathogenesis of systemic lupus erythematosus. *Nat Clin Pract Rheumatol* 2006; **2**:330–7.

42 Gunnarsson I, Sundelin B, Heimburger M, Forslid J, van Vollenhoven R, Lundberg I, Jacobson SH. Repeated renal biopsy in proliferative lupus nephritis – predictive role of serum C1q and albuminuria. *J Rheumatol* 2002; **29**:693–9.

43 Buyon JP, Tamerius J, Belmont HM, Abramson SB. Assessment of disease activity and impending flare in patients with systemic lupus erythematosus. Comparison of the use of complement split products and conventional measurements of complement. *Arthritis Rheum* 1992; **35**:1028–37.

44 Markiewski MM, Lambris JD. The role of complement in inflammatory diseases from behind the scenes into the spotlight. *Am J Pathol* 2007; **171**:715–27.

45 Sturfelt G. The complement system in systemic lupus erythematosus. *Scand J Rheumatol* 2002; **31**:129–32.

46 Holmskov U, Malhotra R, Sim RB, Jensenius JC. Collectins: collagenous C-type lectins of the innate immune defense system. *Immunol Today* 1994; **15**:67–74.

47 Weis WI, Drickamer K, Hendrickson WA. Structure of a C-type mannose-binding protein complexed with an oligosaccharide. *Nature* 1992; **360**:127–34.

48 Takahashi M, Mori S, Shigeta S, Fujita T. Role of MBL-associated serine protease (MASP) on activation of the lectin complement pathway. *Adv Exp Med Biol* 2007; **598**:93–104.

49 Turner MW. Mannose-binding lectin: the pluripotent molecule of the innate immune system. *Immunol Today* 1996; **17**:532–40.

50 Holmskov U, Malhotra R, Sim RB, Jensenius JC. Collectins: collagenous C-type lectins of the innate immune defense system. *Immunol Today* 1994; **15**:67–74.

51 Thiel S, Vorup-Jensen T, Stover CM *et al.* A second serine protease associated with mannan-binding lectin that activates complement. *Nature* 1997; **386**:506–10.

52 Lhotta K, Wurzner R, Konig P. Glomerular deposition of mannose-binding lectin in human glomerulonephritis. *Nephrol Dial Transplant* 1999; **14**:881–6.

53 Ohsawa I, Ohi H, Tamano M *et al.* Cryoprecipitate of patients with cryoglobulinemic glomerulonephritis contains molecules of the lectin complement pathway. *Clin Immunol* 2001; **101**:59–66.

54 Trouw LA, Seelen MA, Duijs JM *et al.* Activation of the lectin pathway in murine lupus nephritis. *Mol Immunol* 2005; **42**:731–40.

55 Jorgensen TN, Gubbels MR, Kotzin BL. New insights into disease pathogenesis from mouse lupus genetics. *Curr Opin Immunol* 2004; **16**:787–93.

56 Lauwerys BR, Wakeland EK. Genetics of lupus nephritis. *Lupus* 2005; **14**:2–12.

ぶんせき

別　刷

No. 1　　2010

糖鎖関連医薬品の開発と分析化学

川崎　ナナ

社団法人 日本分析化学会

東京都品川区西五反田1丁目26番2号　五反田サンハイツ304号

講　義

糖鎖関連医薬品の開発と分析化学

抗体医薬品やムコ多糖症治療薬などに代表されるように，様々な糖タンパク質や多糖類が医薬品として利用されている。糖タンパク質及び多糖類の糖鎖の構造は，溶解性，安定性，生物活性，体内動態，及び安全性に影響すること，また，製造細胞・起源や製造方法の変更によって変化することから，品質，有効性及び安全性を確保するためには，糖鎖構造解析及び糖鎖試験法の設定は不可欠である。本稿では，糖鎖関連医薬品開発における糖鎖分析の重要性を，最近話題になった医薬品を例に解説する。

川崎　ナナ

1　はじめに

健康なヒトや動物に由来する多くの糖タンパク質や多糖類，並びに遺伝子組換え技術等により製造された糖タンパク質が世界中で医薬品として利用されている[1)~3)]。生物起源由来の糖鎖関連医薬品の歴史は古く，性腺刺激ホルモン，ウロキナーゼ，カリジノゲナーゼ，ヘパリン，ヒアルロン酸及びコンドロイチン硫酸エステルなどが現在も使用されている。1980年代になって，遺伝子組換え技術や細胞培養技術の進展によりバイオテクノロジー応用医薬品（バイオ医薬品）が開発されるようになり，ヒト細胞由来インターフェロンアルファ，ヒト組織プラスミノーゲン活性化因子と同一アミノ酸配列をもつアルテプラーゼ（遺伝子組換え），及びヒトエリスロポエチンと同一アミノ酸配列をもつエポエチン（遺伝子組換え）類など多くの糖鎖関連バイオ医薬品が開発された。初期に開発されたバイオ医薬品の多くは，ヒト型アミノ酸配列にヒトとは異なる糖鎖が結合した半天然型であったが，最近では，エタネルセプトやダルベポエチンのように，機能性や体内動態プロファイルを改善するために様々な改変や修飾を施した完全非天然型の糖タンパク質が開発されるようになってきた。多くの糖鎖関連医薬品において糖鎖部分の構造は，安定性，有効性及び安全性に直接影響を与えることから，開発段階での構造解析や上市後の品質管理としての糖鎖試験は重要である。本稿では，糖鎖関連医薬品の糖鎖部分の構造と一般的な糖鎖分析法を解説し，最近話題になった糖鎖関連医薬品を例に取り上げながら，糖鎖分析の重要性について概説する。

2　糖鎖関連医薬品の糖鎖の構造と分析法

糖タンパク質医薬品に結合している糖鎖には*N*結合型糖鎖と*O*結合型糖鎖があり，*N*結合型糖鎖はAsn-Xaa-Ser/Thr配列（XaaはPro以外）のAsnに，また，*O*結合型糖鎖はSerまたはThrに結合している。

*N*結合型糖鎖は，2分子の*N*-アセチルグルコサミン（GlcNAc）と3分子のマンノース（Man）からなるコア部分に側鎖が結合した構造をもち，側鎖に占めるManの割合が高いものから，高マンノース型，混成型，及び複合型糖鎖と分類される（図1）[4)]。生体にはMan，マンノース6リン酸，及びガラクトース（Gal）を認識する受容体などが存在し，糖鎖関連医薬品の血中半減期に大きく影響するので，医薬品開発においては，それらとの反応性を明らかにすることが重要である。

*O*結合型糖鎖は複数の型及びコア構造に分類されるが，糖タンパク質医薬品でよく見られる*O*結合型糖鎖は，ムチン型コア1構造をもつ糖鎖である（図1）[4)]。他に，アルテプラーゼやウロキナーゼのように，Thrにフコースが直接結合しているものや，トロンボモジュリンアルファのように，Serにグルコースが結合している医薬品もある。また，グリコサミノグリカンであるヘパリン及びコンドロイチン硫酸エステルも*O*結合型糖鎖の一つであり，コアタンパク質のSerにグルクロン酸-Gal-Gal-キシロースのリンカー部分を介して結合していたものである。

糖タンパク質医薬品の糖鎖部分の分析法として，単糖分析，オリゴ糖分析，糖ペプチド分析，及びグライコフォーム分析の四つの方法がある。単糖分析は，糖鎖を酸加水分解し，遊離した単糖をHPLCやキャピラリー電気泳動法で定量する方法で，分子全体に占める糖鎖の割合，及び糖鎖の型などがわかる。図2は，陰イオン交換クロマトグラフィーパルス式電気化学検出法により得られたエポエチン由来単糖のクロマトグラムで，エポエチン糖鎖の特徴，すなわち，主糖鎖がフコース（Fuc）結合複合型糖鎖であることをよく示している。オリゴ糖分析は，タンパク質から切り出した糖鎖部分をHPLCやキャピラリー電気泳動法により解析する方法で，糖鎖の構造や結合比率の概略がわかる。図3[5)]は，LC/MS

Analytical Chemistry in Development of Glycosylated Biopharmaceuticals.

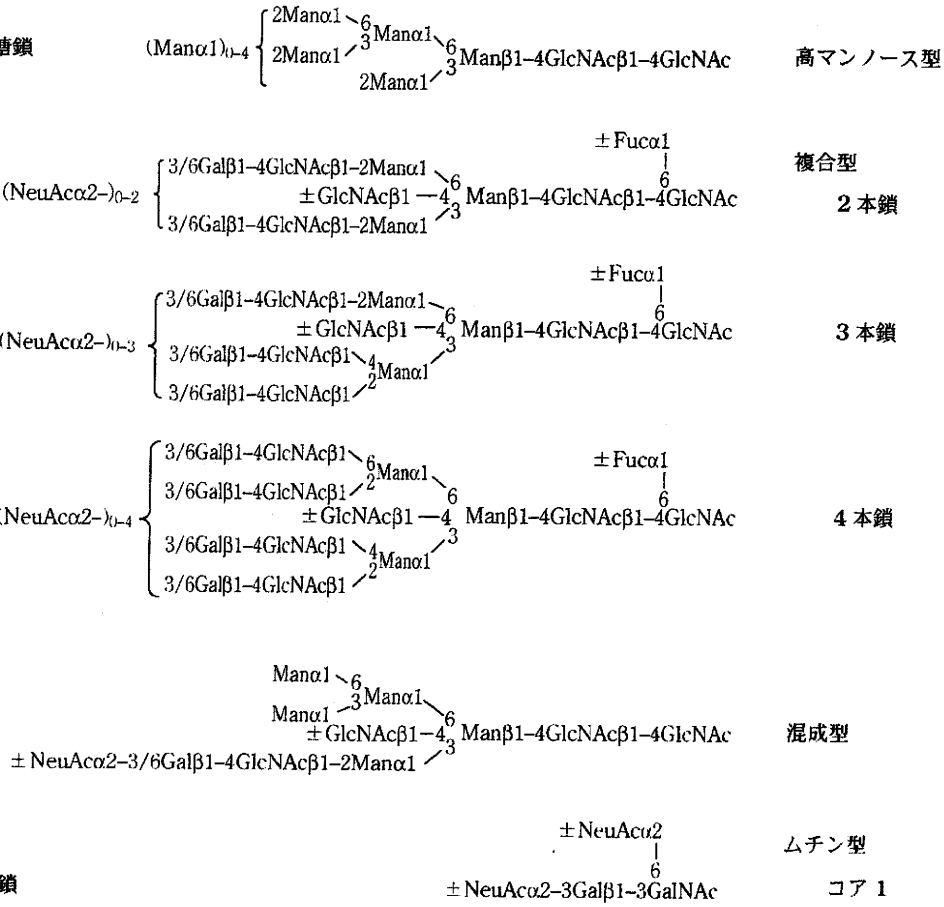

図 1　糖タンパク質医薬品に見られる *N* 結合型糖鎖及び *O* 結合型糖鎖の構造[4]

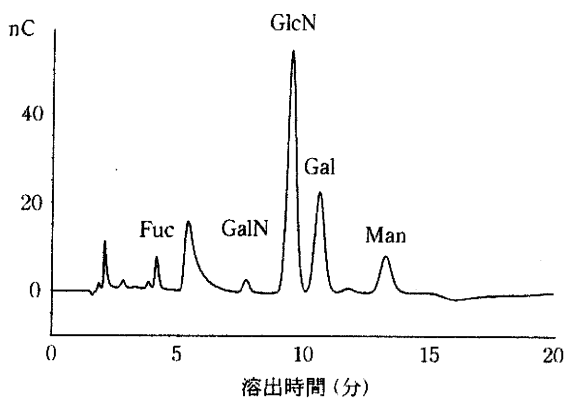

Fuc：フコース，GalN：ガラクトサミン，GlcN：グルコサミン，Gal：ガラクトース，Man：マンノサミン

図 2　**HPAEC-PAD** を用いた単糖組成分析の例（エポエチン酸加水分解物のクロマトグラム）（原園　景博士の提供）

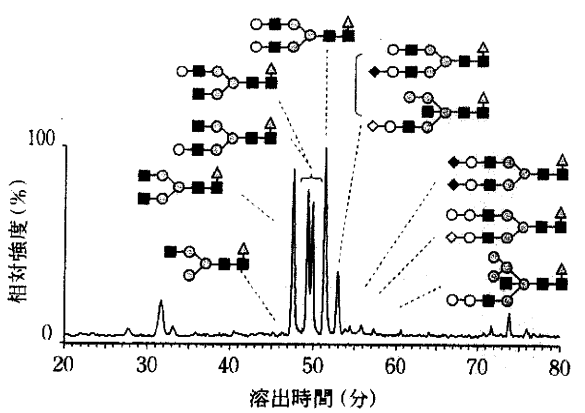

○：Gal，○：Man，■：GlcNAc，△：Fuc

図 3　**LC/MS** を用いた糖鎖プロファイリングの例（抗体医薬品から遊離させた糖鎖のトータルイオンクロマトグラムと帰属[5]）

を用いてある抗体医薬品の *N* 結合型糖鎖を分析した結果で，Gal が 0～2 個結合したフコシル 2 本鎖糖鎖が結合していることがわかる。分子内に複数の糖鎖結合部位が存在するときは，タンパク質を糖ペプチドに断片化し，ペプチドごとの糖鎖の構造と比率を明らかにする。図 4[6]は，抗体医薬品の定常部からトリプシン消化によって生じた *N* 結合型糖鎖結合ペプチドのマススペクトルで，定常部に結合している糖鎖の種類がわかる。グライコフォーム分析は，糖鎖の違いによって生じたアイソフォームの構造と比率を明らかにする方法で，キャピラリー電気泳動，等電点電気泳動，質量分析法などが用いられる。図 5[4]は，あるエポエチンの二次元電気泳動

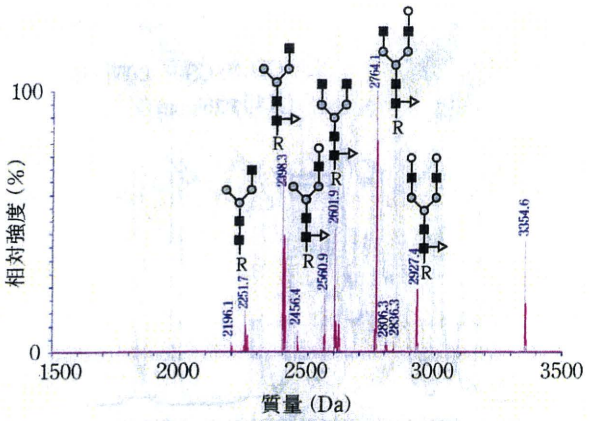

○: Gal, ●: Man, ■: GlcNAc, △: Fuc, R : peptide

図4　MSを用いた糖ペプチド解析の例（抗体医薬品の定常部からトリプシン消化によって生じた糖ペプチドのマススペクトルと帰属[6]）

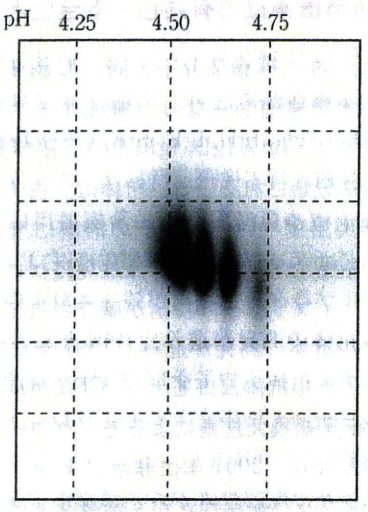

図5　二次元電気泳動を用いたグライコフォーム解析の例（エポエチンの泳動図[4]）

パターンで，分子量及び等電点が異なるグライコフォームの分布がわかる。

グリコサミノグリカンにおいては，各種HPLCやNMRを用いて，構成糖，結合位置，硫酸化の位置や割合を解析する。また，低分子量ヘパリンにおいては，分子量分布や還元末端及び非還元末端の構造を解析する。

通常，糖鎖構造は複雑で不均一性が高いので，一つの方法で特徴を明らかにすることは難しく，医薬品開発段階では，いくつかの方法を組み合わせて解析する。品質管理段階では，糖鎖構造の特徴や，有効性及び安全性に影響する糖鎖構造を考慮して適切な分析法を選択し，試験法として設定する。

3　ムコ多糖症治療薬の有効性と糖鎖

ムコ多糖症は，リソソーム病の一つであり，細胞内小

表1　リソソーム病，原因酵素およびバイオ医薬品[4]

疾　患	原因酵素	治療薬
ムコ多糖症I型	α-L-iduronidase（α-L-イズロニダーゼ）	ラロニダーゼ
ムコ多糖症II型	iduronate-2-sulfatase（イズロン酸-2-スルファターゼ）	イデュルスルファーゼ
ムコ多糖症VI型	*N*-acetylgalactosamine-4-sulfatase（*N*-アセチルガラクトサミン-4-スルファターゼ）	ガルスルファーゼ
糖原病II型（ポンペ病）	α-glucosidase（α-グルコシダーゼ）	アルグルコシダーゼアルファ
ファブリー病	α-galactosidase（α-ガラクトシダーゼ）	アガルシダーゼアルファ アガルシダーゼベータ
ゴーシェ病	β-D-glucocerebrosidase（β-D-グルコセレブロシダーゼ）	アルグルセラーゼ イミグルセラーゼ

器官であるリソソーム内のグリコサミノグリカン加水分解酵素群の一つが低下または欠損することにより，デルマタン硫酸エステル，ヘパラン硫酸エステル，ケラタン硫酸エステル，及びコンドロイチン硫酸エステルなどが組織中に蓄積され，主に骨，内臓，心臓血管，神経系などが障害される疾患である。ムコ多糖症は，活性が低下する酵素の種類に応じてI～VII型（V型欠番）に分類され，欠損する酵素を補う酵素補充療法が行われている（表1）[7]。ムコ多糖症I型及びII型は，それぞれデルマタン硫酸エステル分解酵素α-L-イズロニダーゼ及びイズロン酸-2-スルファターゼの欠損により発症する病気で，治療薬としてそれぞれラロニダーゼ及びイデュルスルファーゼが用いられている。デルマタン硫酸エステル及びコンドロイチン硫酸エステルの分解にかかわる*N*-アセチルガラクトサミン4-スルファターゼが欠損すると，ムコ多糖症VI型を発症する。治療薬としてガルスルファーゼが承認されている。

リソソーム内にはムコ多糖症原因酵素以外にも，複合糖質及び脂質を分解する様々な酵素が存在しており，そのいずれかが欠損すると別のリソソーム病を発症する。現在，約30種類のリソソーム病が知られており，我が国では，ポンペ病治療薬アルグルコシダーゼ アルファ，ファブリー病治療薬アガルシダーゼ アルファ及びアガルシダーゼ ベータ，並びにゴーシェ病治療薬アルグルセラーゼ及びイミグルセラーゼが承認されている（表1）[7]。

リソソーム酵素にはマンノース6リン酸が結合した高マンノース型糖鎖が結合しており，酵素はマンノース6リン酸受容体を介してリソソーム内に取り込まれて効果を発揮する。遺伝子組換えリソソーム酵素医薬品の開発及び品質管理では，糖鎖構造を明らかにすることと，活性に関与するマンノース6リン酸結合糖鎖の構造と

結合比率の恒常性を担保できる規格及び試験法を設定することが必須である。また，イミグルセラーゼのように，マクロファージへの取り込みを助けるため糖鎖の非還元末端がManにまでトリミングされている医薬品においては，その確認が必要である。

4　ヘパリン危機と試験法

ヘパリンナトリウムは，血栓塞栓症の治療や透析の際の抗凝固剤として世界中で古くから利用されている医薬品である。ヘパリンは，*N*-アセチルまたは*N*-硫酸化グルコサミンとイズロン酸またはグルクロン酸の2糖単位の繰り返しからなるグリコサミノグリカンで，2糖単位あたり平均2～2.5個の水酸基が硫酸化されている。これまで大規模な有害事象は報告されてこなかったが，2007年秋，主に米国において，ヘパリンナトリウムの大量静脈投与により，200名以上もの患者が死亡する重大な有害事象が発生した[8]。原因物質として，ヘパリンに含まれていた非天然型多糖類であるover-sulfated chondroitin sulfate (OSCS) が特定された。OSCSは，*N*-アセチルガラクトサミンとグルクロン酸からなり，2糖単位あたり四つの硫酸エステル基を持ち，抗凝固活性を示す物質である[9,10]。ヘパリンは世界規模で利用されている医薬品であり，OSCSが混入したヘパリンは日米欧を含む世界中に広がっていたため，国際的に深刻なヘパリン不足が懸念された（ヘパリン危機）。各国の規制当局及びヘパリン製造販売業者は，直ちにOSCSのスクリーニングによるヘパリン製剤の安全性確認を行い，OSCSが混入されていないヘパリンの供給に努めた。このとき採用されたスクリーニング法は，^{1}H-NMRを用いた方法と，キャピラリー電気泳動を用いた方法であった。^{1}H-NMRは，ヘパリンを構成する*N*-アセチルグルコサミンのアセチル基のプロトンと，OSCSを構成する*N*-アセチルガラクトサミンの*N*-アセチル基のプロトンの化学シフトがそれぞれ2.04及び2.15 ppmと異なることを利用した方法である（図6）[11]。この方法は直ちに日本薬局方，米国薬局方及び欧州薬局方にも取り入れられることとなった。

このヘパリン問題により，ヘパリンを抗凝固活性のみにより規定してきた各国の試験法の問題点が明らかとなり，各国は，安全なヘパリンの安定供給をめざして，理化学的試験法の導入を検討することとなった。その一つは，^{1}H-NMRによりヘパリンの主要構成単糖，結合様式，硫酸化の位置を確認する方法であり，この試験法が採用されれば，ヘパリンと他の多糖類を構造の面から明確に区別できるようになる。もう一つの方法は，陰イオン交換HPLCによる硫酸化程度の確認で，2糖単位あたり2～2.5個の水酸基が硫酸化されていることを確認できるようになる。

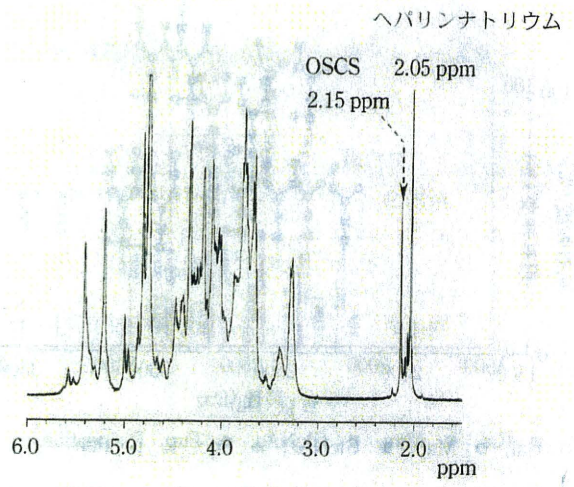

図6　^{1}H-NMRを用いた多糖類の純度試験の例（OSCSが混入したヘパリンナトリウムの^{1}H-NMRスペクトル[11]）

5　抗体医薬品の有効性・安全性と糖鎖

抗体は，同一H鎖2分子と同一L鎖2分子から構成される4本鎖構造からなり，構成するポリペプチド鎖の違いにより，IgG, IgD, IgE, IgA，及びIgMの5種類のクラスに分類される[12,13]。抗体は，古くからウイルス性劇症肝炎治療や免疫不全症の治療に用いられてきたが，ほとんどはポリクローナルな免疫グロブリン製剤であった。ハイブリドーマ技術が確立されてからは，モノクローナル抗体の開発が進み，1991年には国内最初のモノクローナル抗体ムロモナブ-CD3が承認された。さらに，遺伝子組換え技術によるモノクローナル抗体の作製が可能となり，2001年に非ホジキンリンパ腫治療薬リツキシマブ及び転移性乳がん治療薬トラスツズマブが承認されて以降，国内では2009年7月現在までに13品目（米国では21品目，EUでは16品目）の遺伝子組換えモノクローナル抗体が承認されている。なお，世界保健機構（WHO）が定める医薬品国際一般名（INN）には，実に170品目を超える抗体医薬品が収載されている[14,15]。

医薬品として開発されている抗体はIgG及びIgMであるが，現在までに日米欧で承認されている抗体医薬品はIgGのみである。IgG抗体はIgG1, IgG2, IgG3及びIgG4の四つのサブクラスに分類されるが，国内では主にIgG1が販売されている。IgG1抗体医薬品は，さらに完全型と断片｛Fab, F(ab')$_2$｝型に分類される（図7）[16]。IgG 1完全抗体の定常部には共通してGalが0～2個結合した*N*結合型2本鎖糖鎖が結合しているが，可変部にAsn-Xaa-Ser/Thr配列が出現したときにも，*N*結合型糖鎖が結合する可能性がある。糖タンパク質としての抗体医薬品開発における重要なポイントは，抗体依存性細胞性細胞傷害（antibody-dependent cell-mediated cytotoxicity; ADCC）活性や補体依存性細胞

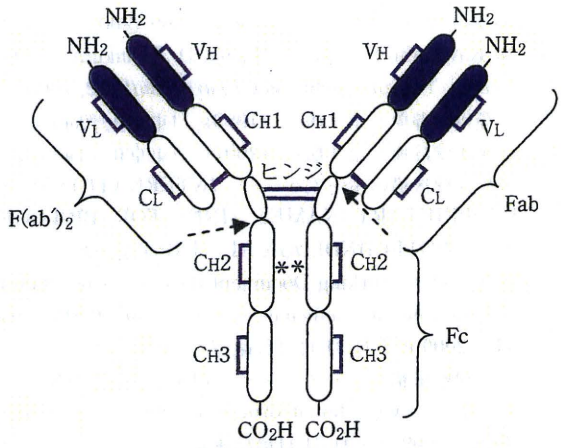

V_L：L鎖可変部，V_H：H鎖可変部，C_L：L鎖定常部，C_H：H鎖定常部，＊：*N*結合糖鎖不加，—：ジスルフィド結合

図7　**IgG1**の構造[16]

傷害（complement－dependent cytotoxicity; CDC）活性があるかどうか，また可変部に糖鎖が付加しているかどうかである。

ADCC活性やCDC活性は，抗腫瘍活性をもつ多くの抗体医薬品に見られる特徴で，定常部に結合している*N*結合型糖鎖の構造に影響されることが報告されている。従って，抗体医薬品の開発にあたって，ADCC活性及びCDC活性の有無を明らかにし，活性が認められる場合は，糖鎖試験を設定すべきである。

可変部に*N*結合型糖鎖が結合したとき，糖鎖構造に製造細胞が持つ特徴が現れることがある。例えば，マウス細胞で製造すると，非ヒト糖鎖抗原 Gal（α1→3）Galが出現することがある。セツキシマブは，結腸・直腸癌治療薬として2008年に承認されたマウス細胞（SP2/0細胞）で製造されるキメラ抗体で，可変部に*N*結合型糖鎖が結合している。この抗体には糖鎖抗原 Gal（α1→3）Galが結合しており，糖鎖部分に反応して過敏症を示す患者がいることが報告されている[17]。

最近，糖鎖構造解析にMSが用いられる傾向があるが，MS単独では各糖鎖の結合比率，構成単糖，及び結合様式がわからないので，注意が必要である。例えば，非ヒト糖鎖抗原［Gal（α1→3）Gal＋GlcNA］を持つ糖鎖は，定常部でよく見られる2本鎖糖鎖［Gal（β1→4）GlcNAc＋Gal］と分子量が同じである。MSのみでは糖鎖の違いを区別できないので，酵素，HPLCやキャピラリー電気泳動等を組み合わせるべきである。

6　製造方法の違いと糖鎖の類似性

糖タンパク質の糖鎖の構造と分布は，製造細胞や組織が発現している糖転移酵素や，培養方法及び精製方法などの製造方法の影響を受けて変動する。前述したように，糖鎖構造の違いは有効性や安全性に影響を及ぼすので，WHOや各国は，アミノ酸配列が同じでも，糖鎖部分が異なる医薬品は，別の医薬品として区別している。例えば，エリスロポエチンは，赤血球前駆細胞に作用して赤血球への分化と増殖を促す造血因子で，3本の*N*－結合型糖鎖と1本の*O*－結合型糖鎖が結合している。糖鎖の非還元末端に結合しているシアル酸の数が多いほど，血中半減期が長くなることが知られている。現在，WHOのINNには，ヒトエリスロポエチンと同一のアミノ酸配列をもち，異なる糖鎖分布を持つ医薬品が10品目登録されている。このうち日本で承認されているのは，エポエチンアルファ及びエポエチンベータであり，この二つは異なる製造販売業者により製造されている。

同一製造業者でも，科学的または経済的理由により，糖タンパク質性医薬品の製造方法を変更することがある。製法変更前後で糖鎖部分の類似性を実証できなければ，同一医薬品として認められないことがある。前述したアルグルコシダーゼ アルファは，ポンペ病治療に用いられる遺伝子組換え糖タンパク質性医薬品で，米国では160 Lスケールで製造された製剤がMyozymeの商品名で販売されていた。供給量を増加させるために製造スケールを2000 Lに上げたところ，米国食品医薬品局（FDA）よりMyozymeとして販売する許可が得られなかった。これは製造スケールを変えたことにより，糖鎖構造が変化したことが理由である[18]。

異なる製造販売業者により，国内で既に承認されたバイオ医薬品と同等/同質の品質，安全性，有効性を有するものとして開発される医薬品は，バイオ後続品と呼ばれる[19,20]。1980～1990年代に開発された多くの既承認薬の独占的販売期間が過ぎたことから，製造コストの抑制が期待されるバイオ後続品開発への関心が世界規模で高まっている。EUでは成長ホルモンであるソマトロピンなどに続き，すでに5種類のエポエチンアルファのバイオ後続品製剤が承認されている。バイオ後続品が糖タンパク質である場合，既承認薬との糖鎖の類似性を検証することが重要である。

7　おわりに

医療用医薬品売上げに占めるバイオ医薬品の割合は年々増加しており，この傾向は今後ますます続くと思われる。新薬開発では，抗体医薬品や融合タンパク質のような遺伝子改変だけでなく，糖鎖改変などによる従来の医薬品との差別化が進むことが予想される。一方で，特許期間が過ぎた既承認の糖タンパク質医薬品のバイオ後続品開発が加速されることも予想されている。また，ヘパリンのように医療上欠かせない生物起源由来医薬品は，今後も引き続き安定供給が求められるであろう。従って，候補糖タンパク質の中から素早く的確に最適な糖タンパク質を選別する技術，糖鎖の構造と機能を十分に理解するための分析技術，並びに有効性と安全性を担保できる定量的糖鎖分析法の開発が今後一層求められる

ことになると思われる。

文　献

1) 第15改正日本薬局方（厚生労働省）
2) 独立行政法人医薬品医療機器総合機構のホームページ：医療用医薬品の添付文書情報 http://www.info.pmda.go.jp/info/pi_index.html（2009年7月31日最終確認）
3) 米国食品医薬品局のホームページ：FDA Drug information-Product approval information-http://www.fda.gov/cder/drug/default.htm（2009年7月31日最終確認）
4) 川崎ナナ，早川堯夫："バイオ医薬品の開発と品質・安全性確保"，早川堯夫監修，p308-329（2007），（エル・アイ・シー）
5) 川崎ナナ，伊藤さつき，山口照英："抗体医薬の最前線"，植田充美監修 p105-115（2007），（シー・エム・シー出版）
6) 川崎ナナ，石井明子，山口照英，荒戸照世："抗体医薬品における規格試験法・製造と承認申請" p. 119-132（2009），（サイエンス&テクノロジー）．
7) 川崎ナナ，内田恵理子，宮田直樹：*Pharm. Tech. Jpn*, **24**, 651（2008）．
8) 米国薬局方のホームページ，http://www.usp.org/hottopics/heparin.htm（2009年7月31日最終確認）
9) T. K. Kishimoto, K. Viswanathan, T. Ganguly, S. Elankumaran, S. Smith, K. Pelzer, J. C. Lansing, N. Sriranganathan, G. Zhao, Z. Galcheva-Gargova, A. Al-Hakim, G. S. Bailey, B. Fraser, S. Roy, T. Rogers-Cotrone, L. Buhse, M. Whary, J. Fox, M. Nasr,, G. J. Dal Pan, Z. Shriver, R. S. Langer, G. Venkataraman, K. F. Austen, J. Woodcock, R. Sasisekharan: *N. Engl. J. Med.*, **358**, 2457（2008）．
10) M. Guerrini, D. Beccati, Z. Shriver, A. Naggi, K. Viswanathan, A. Bisio, I. Capila, J. C. Lansing, S. Guglieri, B. Fraser, A. Al-Hakim, N. S. Gunay, Z. Zhang, L. Robinson, L. Buhse, M. Nasr, J. Woodcock, R. Langer, G. Venkataraman, R. J. Linhardt, B. Casu, G. Torri, and R. Sasisekharan: *Nat. Biotechnol.* **26**, 669（2008）．
11) N. Kawasaki, S. Itoh, N. Hashii, D. Takakura, Y. Qin, H. Xiaoyu, T. Yamaguchi: *Biol. Pharm. Bull.*, **32**, 796（2009）．
12) "免疫学辞典，第1版"，（1993），（東京化学同人）．
13) "生化学辞典，第4版"，（2007），（東京化学同人）．
14) 世界保健機構のホームページ：INTERNATIONAL NONPROPRIETARY NAMES（INN）FOR BIOLOGICAL AND BIOTECHNOLOGICAL SUBSTANCES（A REVIEW），INN Working Document 05.179, 15/06/2006 http://www.who.int/medicines/services/inn/BioRevforweb.pdf（2009年7月31日最終確認）
15) 世界保健機構のホームページ：pINNおよびrINNのリスト，http://www.who.int/druginformation/general/innlists.shtml（2009年7月31日最終確認）
16) 川崎ナナ，内田恵理子，宮田直樹：*Pharm. Tech. Jpn.*, **23**, 81（2007）．
17) C. H. Chung, B. Mirakhur, E. Chan, Q. T. Le, J. Berlin, M. Morse, B. A. Murphy, S. M. Satinover,, J. Hosen, D. Mauro, R. J. Slebos, Q. Zhou, D. Gold, T. Hatley, D. J. Hicklin, T. A. Platts-Mills: *N Engl J Med.*, **358**, 1109（2008）．
18) G. Mack: *Nat Biotechnal.* **592**, 26（2008）．
19) H. Schellekens: *Nat. Biotechnol*, **22**, 1357（2004）．
20) C. K. Schneider, U. Kalinke: *Nat. Biotechnol.*, **26**, 985（2008）．

川崎ナナ（Nana KAWASAKI）
国立医薬品食品衛生研究所（〒158-8501 東京都世田谷区上用賀1-18-1）。北海道大学大学院修了。薬学博士。≪現在の研究テーマ≫生物薬品の特性解析法の開発。≪趣味≫ガーデニング。
E-mail：nana@nihs.go.jp

STEM CELLS
EMBRYONIC STEM CELLS/INDUCED PLURIPOTENT STEM CELLS

Efficient Adipocyte and Osteoblast Differentiation from Mouse Induced Pluripotent Stem Cells by Adenoviral Transduction

KATSUHISA TASHIRO,[a,b] MITSURU INAMURA,[a,b] KENJI KAWABATA,[b] FUMINORI SAKURAI,[b] KOICHI YAMANISHI,[a,c] TAKAO HAYAKAWA,[d,e] HIROYUKI MIZUGUCHI[a,b]

[a]Graduate School of Pharmaceutical Sciences, Osaka University, Osaka, Japan; [b]Laboratory of Gene Transfer and Regulation, National Institute of Biomedical Innovation, Osaka, Japan; [c]National Institute of Biomedical Innovation, Osaka, Japan; [d]Pharmaceutics and Medical Devices Agency, Tokyo, Japan; [e]Pharmaceutical Research and Technology Institute, Kinki University, Osaka, Japan

Key Words. Adenovirus • Differentiation • Gene expression • Induced pluripotent stem cells

ABSTRACT

Induced pluripotent stem (iPS) cells, which are generated from somatic cells by transducing four genes, are expected to have broad application to regenerative medicine. Although establishment of an efficient gene transfer system for iPS cells is considered to be essential for differentiating them into functional cells, the detailed transduction characteristics of iPS cells have not been examined. Previously, by using an adenovirus (Ad) vector containing the elongation factor-1α (EF-1α) and the cytomegalovirus enhancer/β-actin (CA) promoters, we developed an efficient transduction system for mouse embryonic stem (ES) cells and their aggregate form, embryoid bodies (EBs). In this study, we applied our transduction system to mouse iPS cells and investigated whether efficient differentiation could be achieved by Ad vector-mediated transduction of a functional gene. As in the case of ES cells, the Ad vector containing EF-1α and the CA promoter could efficiently transduce transgenes into mouse iPS cells. At 3,000 vector particles/cell, 80%–90% of iPS cells expressed transgenes by treatment with an Ad vector containing the CA promoter, without a decrease in pluripotency or viability. We also found that the CA promoter had potent transduction ability in iPS cell-derived EBs. Moreover, exogenous expression of a *PPARγ* gene or a *Runx2* gene into mouse iPS cells by an optimized Ad vector enhanced adipocyte or osteoblast differentiation, respectively. These results suggest that Ad vector-mediated transient transduction is sufficient to increase cellular differentiation and that our transduction methods would be useful for therapeutic applications based on iPS cells. STEM CELLS *2009;27:1802–1811*

Disclosure of potential conflicts of interest is found at the end of this article.

INTRODUCTION

Because embryonic stem (ES) cells, derived from the inner cell mass of mammalian blastocysts, can be cultured indefinitely in an undifferentiated state and differentiate into various cell types [1, 2], ES cells have been regarded as a potential source of specific cell populations for cell replacement therapy. However, there are two important issues that must be addressed before ES cells can be applied for regenerative medicine: one is the ethical issue about the use of embryos, and the other is the risk of immune rejection after transplantation. In 2006, Takahashi and Yamanaka [3] reported that ES cell-like pluripotent cells, designated as induced pluripotent stem (iPS) cells, could be generated from mouse skin fibroblasts by retroviral transduction of four genes (POU domain class 5 transcription factor 1 [*Oct-3/4*], SRY-box containing box 2 [*Sox2*], cellular myelocytomatosis oncogene [c-*Myc*], and Kruppel-like factor 4 [*Klf4*]). A recent study demonstrated that iPS cells possessed mostly the same characteristics as ES cells, such as global gene expression [4], DNA methylation [5], and histone modification [6]. Furthermore, iPS cells give rise to adult chimeric offspring and show competence for germline transmission [4–6]. Because iPS cells not only have the properties as described above but also can overcome the ethical concerns and problems with immune rejection and because human iPS cells can also be generated from somatic cells [7–10], they are expected to be applicable to regenerative medicine in place of ES cells.

To apply iPS cells to regenerative medicine, establishing methods for the differentiation of iPS cells into pure functional cells is indispensable. Among the many methods for promoting cellular differentiation, genetic manipulation is one of the most powerful techniques, because overexpression of a

Author contributions: K.T.: conception and design, collection and assembly of data, data analysis and interpretation, manuscript writing, final approval of manuscript; M.I.: collection and assembly of data, final approval of manuscript; K.K. and H.M.: conception and design, financial support, manuscript writing, final approval of manuscript; F.S., K.Y., and T.H.: conception and design, final approval of manuscript.

Correspondence: Hiroyuki Mizuguchi, Ph.D., Department of Biochemistry and Molecular Biology, Graduate School of Pharmaceutical Sciences, Osaka University, 1-6 Yamadaoka, Suita, Osaka 565-0871, Japan. Telephone: +81-6-6879-8185; Fax: +81-6-6879-8185; e-mail: mizuguch@phs.osaka-u.ac.jp Received November 25, 2008; accepted for publication April 23, 2009; first published online in STEM CELLS *EXPRESS* April 30, 2009. 1066-5099/2009/$30.00/0 doi: 10.1002/stem.108

differentiation-associated gene in the cells is considered to direct the cell fate from stem cells into functional cells. Many studies have reported that gene transfer into stem cells promoted their differentiation into functional differentiated cells, including hematopoietic cells [11], pancreatic cells [12], and neurons [13].

Adenovirus (Ad) vectors are some of the most efficient gene delivery vehicles and have been widely used in both experimental studies and clinical trials [14, 15]. Ad vectors are an attractive vehicle for gene transfer because they are easily constructed, can be prepared in high titers, and provide efficient transduction in both dividing and nondividing cells. We have developed efficient methods for Ad vector-mediated transduction into mouse ES cells and their aggregate form, embryoid bodies (EBs) [16, 17]. We also showed that adipocyte differentiation from mouse ES cells was markedly promoted by use of the Ad vector for transient transduction of the peroxisome proliferator-activated receptor γ (*PPARγ*) gene [17], which is known to play essential roles in adipogenesis [18, 19].

Because our transduction method using an optimized Ad vector was effective for enhancing the differentiation of mouse ES cells into target cells, we attempted to apply this system to mouse iPS cells and examined whether the adipocyte and osteoblast differentiation potential of mouse iPS cells could be increased by using Ad vector. In all studies, mouse ES cells were used as a control for comparison with mouse iPS cells. By comparing the promoter activity in mouse iPS cells, we successfully developed a suitable Ad vector for gene transfer into mouse iPS cells. We also found that adipocyte and osteoblast differentiation from mouse iPS cells could be facilitated by Ad vector-mediated transient transduction of a *PPARγ* gene and a runt-related transcription factor 2 (*Runx2*) gene, respectively.

Materials and Methods

Adenovirus Vectors

Ad vectors were constructed by an improved in vitro ligation method [20, 21]. The shuttle plasmids pHMCMV5, pHMCA5, and pHMEF5, which contain the cytomegalovirus (CMV) promoter, the CMV enhancer/β-actin promoter with β-actin intron (CA) promoter (a kind gift from Dr. J. Miyazaki, Osaka University, Osaka, Japan) [22], and the human elongation factor-1α (EF-1α) promoter, respectively, were constructed previously [16, 21]. The *mCherry* gene, which is derived from pmCherry (Clontech, Mountain View, CA, http://www.clontech.com), was inserted into pHMCMV5, pHMCA5, and pHMEF5, resulting in pHMCMV-mCherry, pHMCA-mCherry, and pHMEF-mCherry, respectively. pHMCMV-mCherry, pHMCA-mCherry, or pHMEF-mCherry was digested with I-*Ceu*I/PI-*Sce*I and ligated into I-*Ceu*I/PI-*Sce*I-digested pAdHM4 [20], resulting in pAd-CMV-mCherry, pAd-CA-mCherry, or pAd-EF-mCherry, respectively. Ad-CMV-mCherry, Ad-CA-mCherry, and Ad-EF-mCherry were generated and purified as described previously [17]. The Rous sarcoma virus (RSV) promoter-, the CMV promoter-, the CA promoter-, or the EF-1α promoter-driven β-galactosidase (LacZ)-expressing Ad vector (Ad-RSV-LacZ, Ad-CMV-LacZ, Ad-CA-LacZ, or Ad-EF-LacZ, respectively), the CA promoter-driven mouse PPARγ2-expressing Ad vector (Ad-CA-PPARγ2), the CA promoter-driven mouse Runx2-expressing Ad vector (Ad-CA-Runx2), and a transgene-deficient Ad vector (Ad-null), were generated previously [16, 17, 23, 24]. The vector particle (VP) titer and biological titer were determined by using a spectrophotometric method [25] and by means of an Adeno-X Rapid Titer Kit (Clontech), respectively. The ratios of the biological-to-particle titer were 1:31 for Ad-CMV-mCherry, 1:20 for Ad-CA-mCherry, 1:28 for Ad-EF-mCherry, 1:14 for Ad-CA-LacZ, 1:22 for Ad-EF-LacZ, 1:41 for Ad-RSV-LacZ, 1:21 for Ad-CMV-LacZ, 1:8 for Ad-CA-PPARγ2, 1:17 for Ad-CA-Runx2, and 1:11 for Ad-null.

Mouse ES and iPS Cell Cultures

Three mouse iPS cell clones 20D17, 38C2, and stm99-1 (a kind gift from Dr. S. Yamanaka, Kyoto University, Kyoto, Japan) were used in the present study (20D17 was purchased from Riken BioResource Center, Tsukuba, Japan, http://www.brc.riken.jp) [4, 26]. 20D17 and 38C2, both of which carry Nanog promoter-driven green fluorescent protein (GFP)/internal ribosomal entry site/puromycin-resistant gene, were generated from mouse embryonic fibroblasts (MEFs) [4], and stm99-1, carrying the Fbx15 promoter-driven β-geo cassette (a fusion of the β-galactosidase and neomycin resistance genes), was generated from gastric epithelial cells [26]. These mouse iPS cells and mouse E14 ES cells were routinely cultured in leukemia inhibitory factor-containing ES cell medium (Speciality Media) on mitomycin C-treated MEFs, and iPS cell lines and ES cells were passaged every 2nd day using 0.25% trypsin-EDTA (Invitrogen, Carlsbad, CA, http://www.invitrogen.com). Mouse iPS cells 20D17 and E14 ES cells were also cultured on a gelatin-coated dish. To obtain GFP-expressing undifferentiated cells, iPS cells 20D17 were cultured in ES cell medium containing 1.5 μg/ml puromycin (Sigma-Aldrich, St. Louis, MO, http://www.sigmaaldrich.com) on a gelatin-coated dish. Mouse iPS cell clone 20D17 was used in this report except where otherwise indicated. EB formation from mouse ES and iPS cells was induced using the hanging drop method as described previously [17].

LacZ Assay

Mouse ES cells or iPS cells (5×10^4 cells) were plated on 24-well plates. On the following day, they were transduced with each Ad vector (Ad-null, Ad-RSV-LacZ, Ad-CMV-LacZ, Ad-CA-LacZ, or Ad-EF-LacZ) at 3,000 VPs/cell for 1.5 hours. At 24 hours after incubation, X-galactosidase (Gal) staining was performed as described previously [16]. ES cell-derived EBs (ES-EBs) or iPS cell-derived EBs (iPS-EBs) cultured for 5 days (5d-ES-EBs or 5d-iPS-EBs, respectively) were transduced with each Ad vector at 3,000 VPs/cell. Two days later, LacZ expression was measured by X-Gal staining and β-Gal luminescence assays.

mCherry Expression Analysis

Mouse ES cells or iPS cells were plated on gelatin-coated 24-well plates. On the following day, they were transduced with the indicated dose of Ad-CA-mCherry or Ad-EF-mCherry for 1.5 hours. Twenty-four hours later, mCherry expression was analyzed by flow cytometry on an LSR II flow cytometer using FACSDiva software (BD Biosciences, Tokyo, Japan, http://www.bdbiosciences.com). To transduce the EB interior, the ES-EBs or iPS-EBs were transduced with 3,000 VPs/cell of Ad-CMV-mCherry or Ad-CA-mCherry three times on days 0, 2, and 5 (hereinafter referred to as triple transduction) [17]. In brief, 0d-ES-EBs or 0d-iPS-EBs (ES or iPS cell suspension, respectively) were transduced with Ad vector at 3,000 VPs/cell in a hanging drop for 2 days, and 2d-ES-EBs or 2d-iPS-EBs and 5d-ES-EBs or 5d-iPS-EBs were transduced with the same Ad vector at 3,000 VPs/cell for 1.5 hours. On day 7, mCherry expression in the ES-EBs or iPS-EBs was visualized via confocal microscopy (Leica TCS SP2 AOBS; Leica Microsystems, Tokyo, Japan, http://www.leica.com). The ES-EBs or iPS-EBs were then trypsinized and analyzed for mCherry expression by flow cytometry.

Expression of Coxsackievirus and Adenovirus Receptors

For detection of coxsackievirus and adenovirus receptor (CAR) expression, ES and iPS cells, both of which were cultured on gelatin-coated dishes, were harvested by using phosphate-buffered saline (PBS) containing 1 mM EDTA. Cells were then reacted

with rat anti-mouse CAR monoclonal antibody (kindly supplied from Dr. T. Imai, KAN Research Institute, Hyogo, Japan) and stained with phycoerythrin-labeled donkey anti-rat IgG (Jackson Immunoresearch Laboratories, West Grove, PA, http://www.jacksonimmuno.com). CAR expression was analyzed by using an LSR II flow cytometer.

In Vitro Differentiation

Two days after culture with a hanging drop, the EBs were transferred into a Petri dish and maintained for 3 days in suspension culture in differentiation medium (Dulbecco's modified Eagle's medium [Wako Chemical, Osaka, Japan, http://www.wako-chem.co.jp/english] supplemented with 15% fetal calf serum [Specialty Media, Inc., Phillipsburg, NJ, http://www.millipore.com], 0.1 mM 2-mercaptoethanol [Nacalai Tesque, Kyoto, Japan, http://www.nacalai.co.jp.en], 1× nonessential amino acid [Specialty Media, Inc.], 1× nucleosides [Specialty Media, Inc.], 2 mM L-glutamine [Invitrogen], and penicillin/streptomycin [Invitrogen]) containing 100 nM all-*trans*-retinoic acid (RA) (Wako Chemical) and then cultured for 2 more days in differentiation medium without RA [27, 28]. The cells were transduced with 3,000 VPs/cell of Ad vector (Ad-CA-LacZ, Ad-CA-PPARγ2, or Ad-CA-Runx2) at days 0, 2, and 5 as described above and plated on a gelatin-coated dish on day 7. For adipogenic or osteoblastic differentiation, cells were cultured in differentiation medium containing adipogenic supplements (0.1 M 3-isobutyl-L-methylxanthine [Sigma-Aldrich], 100 nM insulin [Sigma-Aldrich], 10 nM dexamethasone [Wako Chemical], and 2 nM triiodothyronine [Sigma-Aldrich]) or osteogenic supplements (50 μg/ml ascorbic acid 2-phosphate [Sigma-Aldrich]), 5 mM β-glycerophosphate [Sigma-Aldrich], and 10 nM dexamethasone [Wako Chemical]), respectively.

Biochemical Assays

Cells were cultured with adipogenic or osteogenic supplements for 15 days after plating on gelatin-coated plates. Adipocyte differentiation from mouse ES and iPS cells was evaluated by oil red O staining and glycerol-3-phosphate dehydrogenase (GPDH) activity. The oil red O staining and GPDH assay were performed using a Lipid Assay kit and GPDH Assay kit, respectively (Primary Cell Co., Ltd, Hokkaido, Japan, http://www.primarycell.com), according to the manufacturer's instructions. To detect matrix mineralization in the cells, cells were fixed with 4% paraformaldehyde-PBS and stained with $AgNO_3$ by the von Kossa method. To measure calcium deposition, cells were washed twice with PBS and decalcified with 0.5 M acetic acid, and cell culture plates were rotated overnight at room temperature. Insoluble material was removed by centrifugation. The supernatants were then assayed for calcium concentration with a calcium C-test kit (Wako Chemical). DNA in pellets was extracted using a DNeasy tissue kit (Qiagen, Valencia, CA, http://www1.qiagen.com), and calcium content was then normalized to cellular DNA. For the measurement of alkaline phosphatase (ALP) activity, cells were lysed in 10 mM Tris-HCl (pH 7.5) containing 1 mM $MgCl_2$ and 0.1% Triton X-100, and the lysates were then used for assay. ALP activity was measured using the LabAssay ALP kit (Wako Chemical) according to the manufacturer's instructions. The protein concentration of the lysates was determined using a Bio-Rad assay kit (Bio-Rad, Hercules, CA, http://www.bio-rad.com), and ALP activity was then normalized by protein concentration.

Reverse Transcription-Polymerase Chain Reaction

Total RNA was isolated from various kinds of cell populations with the use of ISOGENE (Nippon Gene, Tokyo, Japan, http://www.nippongene.com). cDNA was synthesized by using SuperScript II reverse transcriptase (RT) (Invitrogen) and the oligo(dT) primer. Polymerase chain reaction (PCR) was performed with the use of KOD Plus DNA polymerase (Toyobo, Osaka, Japan, http://www.toyobo.co.jp/e). The product was assessed by 2% agarose gel electrophoresis followed by ethidium bromide staining. The sequences of the primers used in this study are listed in supporting information Table S1.

Teratoma Formation and Histological Analysis

Mouse iPS cells were transduced with Ad-CA-mCherry at 10,000 VPs/cell for 1.5 hours. After culture for 3 days, mouse iPS cells were suspended at 1×10^7 cells/ml in PBS. Nude mice (8-10 weeks; Nippon SLC, Shizuoka, Japan, http://www.jslc.co.jp) were anesthetized with diethyl ether, and we injected 100 μl of the cell suspension (1×10^6 cells) subcutaneously into their backs. Five weeks later, tumors were surgically dissected from mice. Samples were washed, fixed in 10% formalin, and embedded in paraffin. After sectioning, the tissue was dewaxed in ethanol, rehydrated, and stained with hematoxylin and eosin. This process was commissioned to Applied Medical Research Laboratory (Osaka, Japan).

Results

Mouse iPS Cells Express Coxsackievirus and Adenovirus Receptor

In the present study, we mainly used the mouse iPS cell clone 20D17 [4]. To assess whether iPS cells have properties similar to those of ES cells under the present culture conditions, we initially investigated the expression of cellular marker genes of iPS cells (Fig. 1A). Semiquantitative RT-PCR analysis revealed that Oct-3/4 and Nanog, both of which are undifferentiated markers in ES cells, were strongly expressed in iPS cells. iPS cells also expressed GFP in the undifferentiated state only, because GFP expression was driven by the Nanog promoter [4]. By EB formation, the expression levels of Oct-3/4, Nanog, and GFP in iPS cells were decreased and, in turn, the three germ layer marker genes (ectoderm: nestin and fibroblast growth factor-5; mesoderm: brachyury T and flk-1; and endoderm: GATA-binding protein-6 and α-fetoprotein) were expressed. These results showed that the gene expression patterns of iPS cells were indistinguishable from those of ES cells.

We next examined the expression of CAR, a primary Ad receptor on the cellular surface, in iPS cells, because the expression of CAR is known to be essential for the transduction using the conventional Ad vector [29–31]. We have reported that CAR was highly expressed in mouse ES cells and ES-EBs [16, 17]. RT-PCR and flow cytometric analysis showed that CAR expression was observed in iPS cells and the expression level of CAR in iPS cells and iPS-EBs was equivalent to that in ES cells and ES-EBs, respectively (Fig. 1A, 1B). Notably, the expression of CAR was observed in more than 95% of GFP-expressing undifferentiated iPS cells. These results suggest that iPS cells could be efficiently transduced by using a conventional Ad vector.

Ad Vectors Containing the CA or the EF-1α Promoter Have Potent Transduction Activity in Mouse iPS Cells

To examine the transduction efficiency in iPS cells by using Ad vectors, we prepared LacZ-expressing Ad vectors under the control of four different promoters, the RSV promoter, the CMV promoter, the CA promoter, or the EF-1α promoter (Ad-RSV-LacZ, Ad-CMV-LacZ, Ad-CA-LacZ, or Ad-EF-LacZ, respectively). We also prepared Ad-null, a transgene-deficient Ad vector, as a control vector. ES and iPS cells were transduced with each Ad vector at 3,000 VPs/cell, and LacZ expression in the cells was measured. X-Gal staining showed that Ad-RSV-LacZ- or Ad-CMV-LacZ-transduced ES cells expressed little LacZ, whereas Ad-CA-LacZ- or Ad-EF-